Research Article

Journal of PeptideScience

Received: 28 July 2008 Revised: 1 December 2008 Accepted: 9 December 2008 Published online in Wiley Interscience: 10 February 2009

(www.interscience.com) DOI 10.1002/psc.1120

Effects of dimerization of the cell-penetrating peptide Tat analog on antimicrobial activity and mechanism of bactericidal action

Wan Long Zhu[a,b] and Song Yub Shin[a,b]*

The cell-penetrating peptide Tat (48–60) (GRKKRRQRRRPPQ) derived from HIV-1 Tat protein showed potent antibacterial activity (MIC: 2–8 μM). To investigate the effect of dimerization of Tat (48–60) analog, [Tat(W): GRKKRRQRRRPWQ-NH_2], on antimicrobial activity and mechanism of bactericidal action, its dimeric peptides, di-Tat(W)-C and di-Tat(W)-K, were synthesized by a disulfide bond linkage and lysine linkage of monomeric Tat(W), respectively. From the viewpoint of a weight basis and the monomer concentration, these dimeric peptides displayed almost similar antimicrobial activity against six bacterial strains tested but acted more rapidly against *Staphylococcus aureus* on kinetics of bactericidal activity, compared with monomeric Tat(W). Unlike monomeric Tat(W), these dimeric peptides significantly depolarized the cytoplasmic membrane of intact *S. aureus* cells at MIC and induced dye leakage from bacterial-membrane-mimicking egg yolk L-α-phosphatidylethanolamine/egg yolk L-α-phosphatidyl-DL-glycerol (7 : 3, w/w) vesicles. Furthermore, these dimeric peptides were less effective to translocate across lipid bilayers than monomeric Tat(W). These results indicated that the dimerization of Tat analog induces a partial change in the mode of its bactericidal action from intracellular target mechanism to membrane-targeting mechanism. Collectively, our designed dimeric Tat peptides with high antimicrobial activity and rapid bactericidal activity appear to be excellent candidates for future development as novel antimicrobial agents.

Keywords: cell-penetrating peptide; antimicrobial peptide; Tat (48–60); dimerization; antimicrobial activity; bactericidal mechanism

Introduction

Several cationic antimicrobial peptides (AMPs) with multiple basic Arg residues such as PR-39, bactenecins, and apidaecin have been known to have the cell-penetrating property and the bactericidal activity [1–3]. Their bactericidal activity is due to their ability to inhibit the intracellular functions by penetrating through the microbial membrane, rather than to create pores in the cell surface. A cell-penetrating peptide, Tat (48–60) (GRKKRRQRRRPPQ), derived from membrane-penetrating basic domain of HIV-1 Tat protein also contains multiple Arg residues [4,5]. Cationic and membrane-interacting properties of Tat (48–60) have prompted us to examine its antimicrobial potential against microorganisms. In previous studies, Tat peptide [Tat (47–58)] was found to have potent antimicrobial activity with no hemolytic activity [6,7]. In addition, we found that Tat (48–60) displays a broad spectrum and potent antibacterial activity with MIC value of 2–8 μM.

A comparison of the sequences of AMPs reveals that two types of side chains are essential for antimicrobial activity. The cationic side chains, such as Arg and Lys, are thought to mediate peptide interactions with negatively charged membranes and/or cell walls of Gram-negative bacteria [8,9]. Bulky hydrophobic side chains, such as Leu, Phe, and Trp, occur frequently in AMPs, presumably providing lipophilic anchors that ultimately induce membrane disruption [8,9]. It had been reported that antimicrobial activity of AMPs is governed by positive charge and hydrophobicity of peptides and there should be a proper balance between cationic and hydrophobic residues to avoid toxicity toward mammalian cells [8,9]. Among hydrophobic residues, Trp was known to have strong ability to insert into membranes and to cause the peptides to partition into membranes [10,11]. Furthermore, the addition of positive charges to several AMPs including bovine lactoferrin (LF) and bactenecin *via* *C*-terminal amidation increased their antimicrobial activity [12].

On the basis of these results, we designed and synthesized Tat(W) (GRKKRRQRRRPWQ-NH_2) by $Pro^{59} \rightarrow Trp$ substitution and *C*-terminal amidation to increase antimicrobial activity. The substitution of Pro^{59} by a Trp in the Tat (48–60) is also able to take advantage of the useful spectroscopic properties of tryptophan to distinguish the binding affinity of the designed peptides with model membranes [13,14]. Furthermore, to investigate the effect of dimerization of Tat analog on antimicrobial activity and mechanism of action, we synthesized two disulfide-bond-linked and Lys-linked dimeric molecules [di-Tat(W)-C and di-Tat(W)-K]. Antimicrobial activities of peptides against Gram-positive and Gram-negative bacterial strains as well as hemolytic activities were examined. In addition, the kinetics of the peptides' bactericidal activity was accessed using *Staphylococcus aureus*. Tryptophan fluorescence spectroscopy was used to determine the peptide binding affinities for liposomes that mimic bacterial or eukaryotic membranes. Furthermore, we investigated the

* *Correspondence to: Song Yub Shin, Department of Cellular and Molecular Medicine, School of Medicine, Chosun University, Gwangju 501-759, Korea. E-mail: syshin@chosun.ac.kr*

a *Department of Bio-Materials, Graduate School and Research Center for Proteineous Materials, Chosun University, Gwangju 501-759, Korea*

b *Department of Cellular and Molecular Medicine, School of Medicine, Chosun University, Gwangju 501-759, Korea*

mechanism by which these peptides kill bacteria by measuring its potential to cause the leakage of a fluorescent dye from lipid vesicles, the depolarization of the cytoplasmic membrane potential to *S. aureus* and the translocation across the lipid bilayers.

Materials and Methods

Materials

Rink amide 4-methylbenzhydrylamine (MBHA) resin, Wang-resin, Fmoc-amino acids, and other reagents for peptide synthesis were purchased from Calbiochem-Novabiochem (La Jolla, CA, USA). Egg yolk L-α-phosphatidylcholine (EYPC), egg yolk L-α-phosphatidylethanolamine (EYPE), egg yolk L-α-phosphatidyl-DL-glycerol (EYPG), calcein, gramicidin D (GD), trypsin, and trypsin–chymotrypsin inhibitor were supplied by Sigma Chemical Co. (St. Louis, MO, USA). Dansyl-phosphatidylethanolamine (DNS-PE) was purchased from Avanti Polar Lipids (Alabaster, AL, USA). 3,3′-Dipropylthiadicarbocyanine iodide (diSC_3-5) was obtained from Molecular Probes (Eugene, OR, USA). Buffers were prepared in double glass distilled water.

Peptide Synthesis and Purification

Peptides were prepared using Fmoc-based solid phase method. The peptides were cleaved from the resin by treatment with TFA/H_2O/thioanisole/phenol/ethanedithiol/triisopropylsilane (81.5 : 5 : 5 : 5 : 2.5 : 1, v/v) for 2 h at room temperature. The crude peptides were purified using a C_{18} preparative column (Vydac C_{18}, 20 × 250 mm, 300 Å), and peptide purity were verified using a C_{18} analytical column (Vydac C_{18}, 4.6 × 250 mm, 300 Å). Characterization of the peptides was performed by molecular mass determination using MALDI-TOF MS (Shimadzu, Japan) (Table 1). Peptide content was determined by amino acid analysis (Hitachi Model, 8500 A, Japan).

Synthesis of Dimeric Peptides of Tat(W)

Dimeric peptides, di-Tat(W)-C and di-Tat(W)-K, were synthesized by a single disulfide bond linkage and Lys linkage, respectively (Table 1). Di-Tat(W)-K was prepared by the coupling of Fmoc-Lys(Fmoc)-OH to Rink amide MBHA resin. Di-Tat(W)-C was prepared by incubating the purified monomer (GRKKRRQRRRPWQC-NH_2) in 10% DMSO solution (peptide concentration: 1 mg/ml) for 48 h at room temperature. The disulfide bond formation of monomer was checked by analytical C_{18} column. The purity of Di-Tat(W)-C was >95%. Di-Tat(W)-C had the correct molecular mass (Table 1).

Table 1. Amino acid sequences and calculated and observed molecular mass of the peptides

Peptide	Amino acid sequence	Molecular mass (Da)	
		Calculated	Observed
Tat	GRKKRRQRRRPPQ	1719.0	1719.7
Tat(W)	GRKKRRQRRRPWQ-NH_2	1807.1	1807.9
di-Tat(W)-C	(GRKKRRQRRRPWQC-NH_2)$_2$	3820.5	3821.4
di-Tat(W)-K	(GRKKRRQRRRPWQ)$_2$-K-NH_2	3725.4	3726.5

Circular Dichroism (CD)

CD spectroscopy was performed on a J-720 spectropolarimeter (JASCO Corp., Japan) using a quartz cell of 1-mm path length and 100 µg/ml peptide in 50% TFE or 30 mM SDS in the presence of 10 mM sodium phosphate buffer at pH 7.2 at room temperature. Four scans per sample performed over wavelength range 190–250 nm at 0.1 nm intervals.

Antimicrobial Activity (MIC)

The antibacterial activities of peptides against three Gram-positive bacterial strains (*Bacillus subtilis* [KCTC 3068], *Staphylococcus epidermidis* [KCTC 1917], and *Staphylococcus aureus* [KCTC 1621]), and three Gram-negative bacterial strains (*Escherichia coli* [KCTC 1682], *Pseudomonas aeruginosa* [KCTC 1637], and *Salmonella typhimurium* [KCTC 1926]) were examined by the microdilution method as described previously [15]. Bacterial strains were procured from the Korean Collection for Type Cultures (KCTC) at the Korea Research Institute of Bioscience and Biotechnology (KRIBB, Korea).

Kinetics of Bactericidal Activity

The kinetics of the peptides' bactericidal activity was accessed using *S. aureus* at a peptide concentration of 1–2 µM, which is the MIC against *S. aureus*. The initial density of the cultures was approximately 6 × 10^5 CFU/ml. After 0, 5, 10, 30, 50, 70, or 90 min of exposure to the peptides at 37 °C, 50 µl aliquots of serial tenfold dilution (up to 10^{-3}) of the cultures were plated onto LB agar plates to obtain viability counts. Colonies were counted after incubation at 37 °C for 24 h.

Hemolytic Activity (MHC)

Fresh human red blood cells (hRBCs) were washed three times with PBS (35 mM phosphate buffer, 0.15 M NaCl, pH 7.4) by centrifugation for 7 min at 1000 × *g* and resuspended in PBS. The peptide solutions (serial twofold dilutions in PBS) were added to 100 µl of hRBC suspension [4% (v/v) in final] in PBS to a final volume of 200 µl and incubated for 1 h at 37 °C. Samples were centrifuged at 1000 × *g* for 5 min, and hemoglobin release was monitored by measuring supernatant absorbance at 405 nm with Microplate ELISA Reader. The hemolysis percentage was calculated according to the equation: % hemolysis = $100 \times [(A_{sample} - A_{blank})/(A_{triton} - A_{blank})]$

Preparation of Small Unilamellar Vesicles

Small unilamellar vesicles (SUVs) were prepared with a standard procedure using the required amounts of EYPE/EYPG (7 : 3, w/w) or EYPC/cholesterol (10 : 1, w/w) for tryptophan fluorescence. Dry lipids were dissolved in chloroform in a small glass vessel. Solvents were removed by rotary evaporation to form a thin film on the wall of a glass vessel and lyophilized overnight. Dried thin films were resuspended in Tris–HCl buffer by vortex mixing. Lipid dispersions were sonicated on ice water for 10–20 min with a titanium-tip ultrasonicator until the solution became transparent.

Tryptophan Fluorescence Blue Shift

The fluorescence emission spectrum of tryptophan of peptides was monitored in the presence of vesicles composed of either EYPE/EYPG (7:3 w/w) SUVs or EYPC/cholesterol (10:1 w/w) SUVs. In these fluorometric studies, small SUVs were used to minimize differential light scattering effects [16]. Tryptophan fluorescence measurements were obtained using a model RF-5301PC spectrophotometer (Shimadzu, Japan). Each peptide was added to 3 ml of Tris–HCl buffer (10 mM Tris, 0.1 mM EDTA, 150 mM NaCl, pH 7.4) containing 0.6 mM liposomes (pH 7.4), and the peptide/liposome mixture (molar ratio of 1:200) was allowed to interact at 20 °C for 10 min. The fluorescence was excited at 280 nm, and emission was scanned from 300 to 400 nm.

Dye Leakage

Calcein-entrapped large unilamellar vesicles (LUVs) composed of EYPE/EYPG (7:3, w/w) or EYPC/cholesterol (10:1, w/w) were prepared by vortexing the dried lipid in dye buffer solution (70 mM calcein, 10 mM Tris, 150 mM NaCl, 0.1 mM EDTA, pH 7.4). The suspension was subjected to ten frozen–thaw cycles in liquid nitrogen and extruded 21 times through polycarbonate filters (two stacked 100-nm pore size filters) with a LiposoFast extruder (Avestin, Inc., Canada). Untrapped calcein was removed by gel filtration on a Sephadex G-50 column. The concentration of calcein-entrapped LUVs was determined in triplicate by phosphorus analysis [17]. Calcein leakage from LUVs was monitored by measuring fluorescence intensity at an excitation wavelength of 490 nm and emission wavelength of 520 nm on a model RF-5301PC spectrophotometer. For determination of 100% dye release, 20 µl 10% Triton-X100 in Tris-buffer was added to dissolve the vesicles. The percentage of dye leakage caused by the peptides was calculated as follows:

$$\%\ \text{Dye leakage} = 100 \times [(F - F_0)/(F_t - F_0)] \quad (1)$$

where F is the fluorescence intensity achieved at 5 min after peptide addition, and F_0 and F_t represent fluorescence intensities without the peptides and with Triton X-100, respectively.

Membrane Depolarization

The membrane depolarization activity of individual peptides was determined using intact *S. aureus* cells and membrane-potential-sensitive fluorescent dye $diSC_3$-5 based on the method of Friedrich *et al*. [18]. Briefly, *S. aureus* grown at 37 °C with agitation to the mid-log phase ($OD_{600} = 0.4$) was harvested by centrifugation. Cells were washed twice with washing buffer (20 mM glucose, 5 mM HEPES, pH 7.4) and resuspended to an OD_{600} of 0.05 in similar buffer containing 0.1 M KCl. Subsequently, cells were incubated with 20 nM $diSC_3$-5 until stable reduction of fluorescence was achieved, implying incorporation of the dye into the bacterial membrane. Membrane depolarization was monitored by recording changes in the intensity of fluorescence emission of the membrane-potential-sensitive dye, $diSC_3$-5 ($\lambda_{ex} = 622$ nm, $\lambda_{em} = 670$ nm) after peptide addition. The membrane potential was fully dissipated by adding GD (final concentration of 0.2 nM). The membrane-potential-dissipating activity of the peptides is calculated as follows:

$$\%\ \text{Membrane depolarization} = 100 \times [(F_p - F_0)/(F_g - F_0)] \quad (2)$$

where F_0 is the stable fluorescence value after the addition of the $diSC_3$-5 dye, F_p is the fluorescence value 5 min after peptide addition, and F_g is the fluorescence signal after GD addition.

Translocation

Lipid film (EYPC/EYPG/DNS-PE = 50/45/5, w/w/w) was hydrated with 200 µM trypsin solution in a 10 mM HEPES/45 mM NaCl/1 mM EDTA buffer (pH 7.4), and LUVs were prepared. Trypsin–chymotrypsin inhibitor (2 mM) was added to the same volume of LUV suspension to inactivate the enzyme outside the vesicles. Peptides (peptide concentration = 1 µM) were added to the membranes (lipid concentration = 215 µM). Sensitized dansyl fluorescence at 510 nm was recorded on excitation of the Trp residues at 280 nm. A decrease in fluorescence implied digestion of the fluorescent peptide by the enzyme within the liposomes, that is, internalization of the peptide. F10W-buforin II (TRSSRAGLQW-PVGRVHRLLRK) with $Phe^{10} \rightarrow$ Trp substitution was used in this assay, as reported in previous study [19].

Proteolytic Digestion

Digestion of Tat(W), di-Tat(W)-C, and di-Tat(W)-K by trypsin was carried out using 50 µg/ml peptide and 0.2 µg/ml trypsin in PBS at room temperature. The progress of peptide cleavage after several reaction times ranging from 2 to 30 min was monitored chromatographically using a RP column (Vydac C_{18}, 4.6 × 250 mm, 300 Å).

Results

CD Spectra

To investigate the effect of $Pro^{59} \rightarrow$ Trp substitution of Tat (48–60) on the peptide structure, CD spectra of Tat (47–58) and Tat(W) in membrane-mimicking environments (50% TFE or SDS micelles) were measured by CD spectroscopy. As shown in Figure 1, both Tat (48–60) and Tat(W) exhibit a large negative band near 200 nm characteristic of a random coil conformation. This result suggests that $Pro^{59} \rightarrow$ Trp substitution of Tat (47–60) do not induce a significant alternation on the peptide structure.

Antimicrobial and Hemolytic Activities

As the recent research in which Tat (47–58) (YGRKKRRQRRRD) exerted toxic activity toward all bacterial strains at 5–20 µM of peptide concentration [7], Tat (48–60) (GRKKRRQRRRPPQ) also displayed potent antimicrobial activity with the MIC value of 2–8 µM (Table 2). The little difference on MIC of these two Tat peptides is probably from their different sequence and maybe from the different experimental environments. Noticeably, all Tat analogs displayed increased antimicrobial activity compared with Tat. From the viewpoint of a weight basis and the monomer concentration, two dimeric analogs [di-Tat(W)-C and di-Tat(W)-K] exhibited almost similar antimicrobial activity against six bacterial strains tested, compared with monomeric analog, Tat(W) (Table 2). All peptides did not cause hemolytic activity even at the highest

Table 2. Antimicrobial and hemolytic activities of the peptides

Peptide	MIC[a] (μM)						MHC[b] (μM)
	E. coli	*P. aeruginosa*	*S. typhimurium*	*B. subtilis*	*S. epidermidis*	*S. aureus*	
Tat	2	4	8	4	4	4	>200
Tat(W)	2	2	2	2	2	2	>200
di-Tat(W)-C	1	2	2	1	1	1	>200
di-Tat(W)-K	1	1	1	1	1	1	>200

[a] MIC was determined from three independent experiments performed in triplicate.
[b] Minimal hemolytic concentration (MHC) corresponds to the peptide concentration that induces 5% hemolysis.

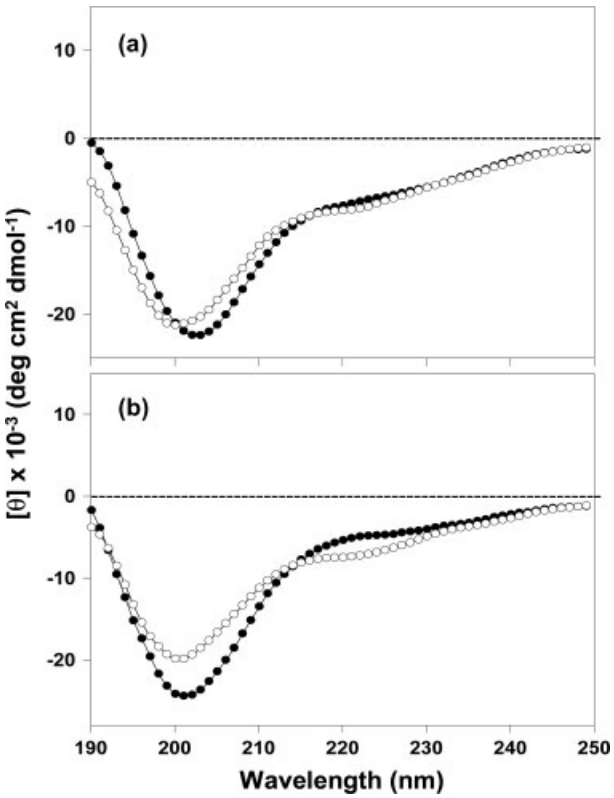

Figure 1. CD spectra of Tat (-●-●-●-●-) and Tat(W) (-○-○-○-○-) in 50% TFE (a) or 30 mM SDS (b) in the presence of 10 mM sodium phosphate buffer (pH 7.2).

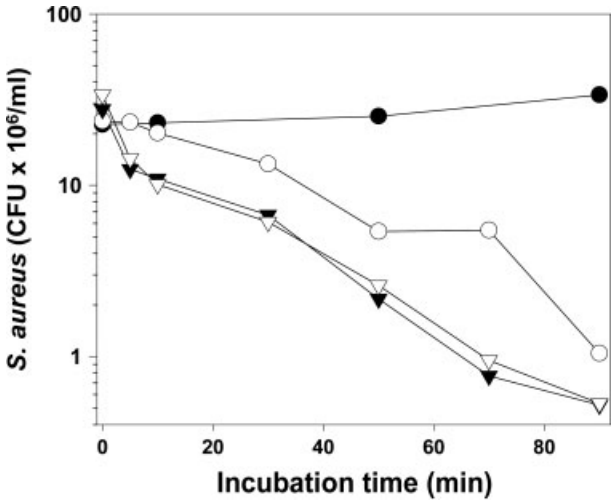

Figure 2. Kinetics of bactericidal activity of the peptides against *S. aureus*. *Staphylococcus aureus* was incubated in the absence (●) and presence of Tat(W) (○), di-Tat(W)-C (▼), or di-Tat(W)-K (▽) in LB broth. The peptide concentration of Tat(W), di-Tat(W)-C, and di-Tat(W)-K was 2, 1, and 1 μM, respectively.

concentration tested (200 μM). To further study the antimicrobial activity of these dimeric analogs [di-Tat(W)-C and di-Tat(W)-K], the kinetics of their bactericidal activity against *S. aureus* was investigated. As shown in Figure 2, these dimeric peptides acted more rapidly than monomeric Tat(W) against *S. aureus* at MIC.

Tryptophan Fluorescence Blue Shift in Model Membranes

When excited at a wavelength of 280 nm, Trp residues in unstructured peptides in aqueous solution give rise to an emission peak centered around 350–355 nm. When the peptide binds the surface of a membrane, the more hydrophobic environment and the decreased flexibility cause the fluorescence emission maxima of peptide to shift to the lower wavelength ('blue shift'). In negatively charged EYPE/EYPG (7:3, w/w) SUVs, all peptides induced a significant blue shift in the fluorescence emission maximum, indicating these peptides penetrate into the hydrocarbon region of anionic lipid bilayer (Table 3). In zwitterionic EYPC/cholesterol (10:1, w/w) SUVs, all peptides caused no blue shift in the fluorescence emission maximum (Table 3). These results correspond well with the results of the biological activity assays (Table 2).

Table 3. Tryptophan emission maxima of 3 μM peptides in Tris-buffer (pH 7.4) or in the presence of 0.6 mM EYPC/EYPG (7:3, w/w) SUVs and 0.6 mM EYPC/cholesterol (10:1, w/w) SUVs

Peptide	Tris-buffer (nm)	EYPE/EYPG (7:3, w/w) (nm)	EYPC/Cholesterol (10:1, w/w) (nm)
Tat(W)	350	339 (11)[a]	350 (0)
di-Tat(W)-C	351	341 (10)	351 (0)
di-Tat(W)-K	350	340 (10)	350 (0)

[a] Blue shift in emission maximum in parentheses.

Membrane Depolarization

To evaluate the effects of peptides on *S. aureus* cytoplasmic membranes, the membrane-potential-sensitive fluorescent dye $diSC_3$-5 was used (Figure 3). This dye is distributed between the

Journal of PeptideScience

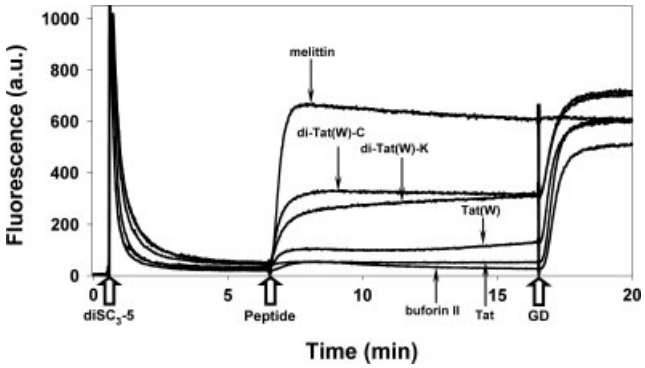

Figure 3. Cytoplasmic membrane depolarization of *S. aureus* ($OD_{600} = 0.05$) by the peptides using the membrane-potential-sensitive dye, $diSC_3$-5. Dye release was monitored at an excitation wavelength of 622 nm and an emission wavelength of 670 nm. GD indicates gramicidin D. The concentration of Tat, Tat(W), di-Tat(W)-C, di-Tat(W)-K, buforin-2, and melittin incubated in *S. aureus* cells was 4, 2, 1, 1, 2, and 0.1 μM, respectively.

cells and the medium, depending on the cytoplasmic membrane potential, and self-quenches when concentrated inside bacterial cells. If the membrane is depolarized, this dye will be released into the medium, causing a measurable increase in fluorescence. Tat and Tat(W) caused no or less membrane depolarization at MIC, as observed in buforin II known as the bacterial-cell-penetrating AMP. On the contrary, dimeric analogs [di-Tat(W)-C and di-Tat(W)-K] caused significant membrane depolarzation of approximately 50% at their MIC. As expected, melittin known as bacterial-cell-disrupting AMP depolarized the cytoplasmic membrane almost completely only at 0.1 μM.

Calcein Leakage from Model Membranes

To examine whether the antimicrobial activities of the peptides depend on their ability to permeate bacterial membranes, we measured their abilities to induce calcein leakage from negatively charged EYPE/EYPG (7 : 3 w/w) LUVs (bacterial-cell-membrane-mimicking environment) (Figure 4). Monomeric Tat and Tat(W) induced weak dye leakage of below 20% at 5 μM, whereas dimeric analog di-Tat(W)-K significantly caused dye leakage of 40% at monomeric peptide concentration of 5 μM. Noticeably, di-Tat(W)-C induced only weak dye leakage of approximately 20% at monomeric peptide concentration of 5 μM, but it caused significant membrane depolarization at its MIC (monomeric peptide concentration: 2 μM). This result is probably because Tat(W)-C forms small channels that permitted transit of ions or protons but not molecules as large as calcein [20,21]. As expected, all peptides showed no dye leakage from zwitterionic EYPC/cholesterol (10 : 1, w/w) LUVs (mammalian-cell-membrane-mimicking environment) at monomeric peptide concentration of 5 μM (Figure 4).

Translocation Across Lipid Bilayers

Translocation of the peptides across lipid bilayers was detected as shown in the previous reports [19]. Trypsin was encapsulated within the internal aqueous phase of EYPC/EYPG/DNS-PE (50/45/5) LUVs to selectively digest the penetrated peptide. The enzyme outside the vesicles was inactivated by trypsin–chymotrypsin inhibitor. The enzyme hydrolyzes the peptide bonds on the *C*-terminal sides of the Lys and Arg residues. The hydrolyzed Trp-containing fragments will be desorbed from the membrane and can be detected by the resonance energy transfer (RET) technique; desorption results in relief of RET, that is, a decrease in dansyl fluorescence at 510 nm when excited at 280 nm, where Trp is selectively excited. The concentration of each peptide used in this experiment is 1 μM. Thus, the monomeric concentration ratio for monomer [Tat(W)] and dimeric analogs [di-Tat(W)-C and di-Tat(W)-K] is 1 : 2. Despite its lower concentration, monomeric analog Tat(W) was translocated across the membrane much more effectively than dimeric analogs [di-Tat(W)-C and di-Tat(W)-K] (Figure 5). The translocation activity of Tat(W) was much closer to that of F10W-buforin II.

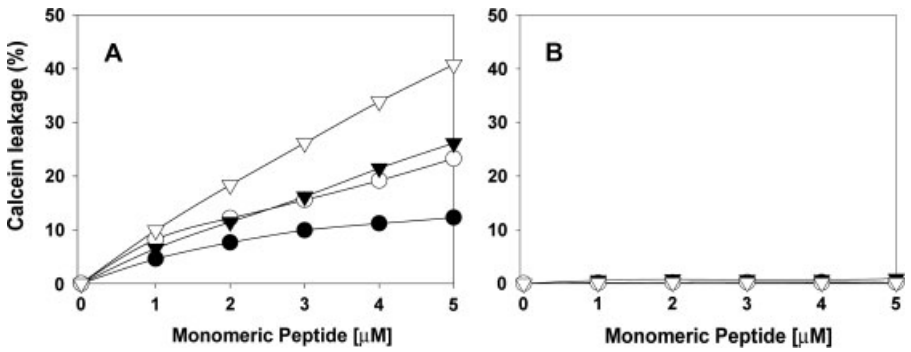

Figure 4. Concentration-dependent peptide-induced calcein release from calcein-entrapped negatively charged EYPE/EYPG (7 : 3, w/w) LUVs (A) or zwitterionic EYPC/cholesterol (10 : 1, w/w) LUVs (B). The percentage of dye leakage caused by the peptides was calculated as follows: % Dye leakage $= 100 \times [(F - F_0)/(F_t - F_0)]$, where F is the fluorescence intensity achieved at 5 min after addition of peptides, F_0 and F_t are fluorescence intensities without the peptides and with Triton X-100, respectively. Peptides are indicated as follows: Tat (●), Tat(W) (○), di-Tat(W)-C (▼), and di-Tat(W)-K (▽).

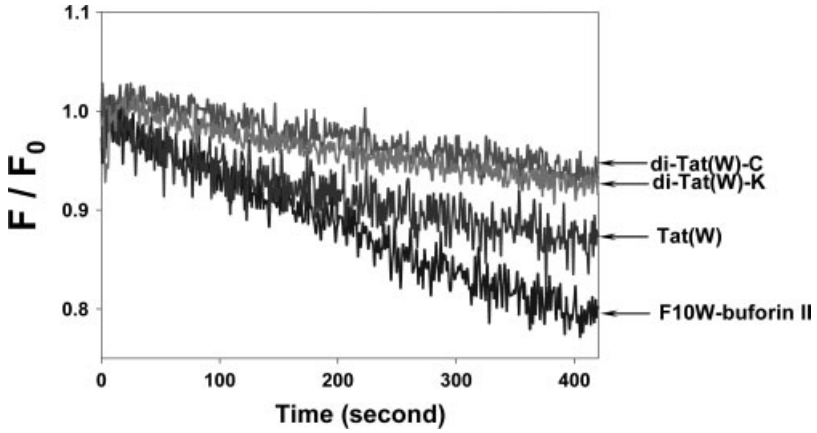

Figure 5. Detection of peptide translocation. The peptides were added to trypsin-entrapping LUVs (EYPC/EYPG/DNS-PE = 50/45/5), and the sensitized dansyl fluorescence at 510 nm was recorded on excitation of Trp residues at 280 nm. Decreases in fluorescence implied digestion of the fluorescent peptide by the enzyme within the liposomes, that is, internalization of the peptide. The peptide concentration was 1 μM. The lipid concentration was 215 μM. The data are expressed as F/F_0, where F_0 is the initial fluorescence value.

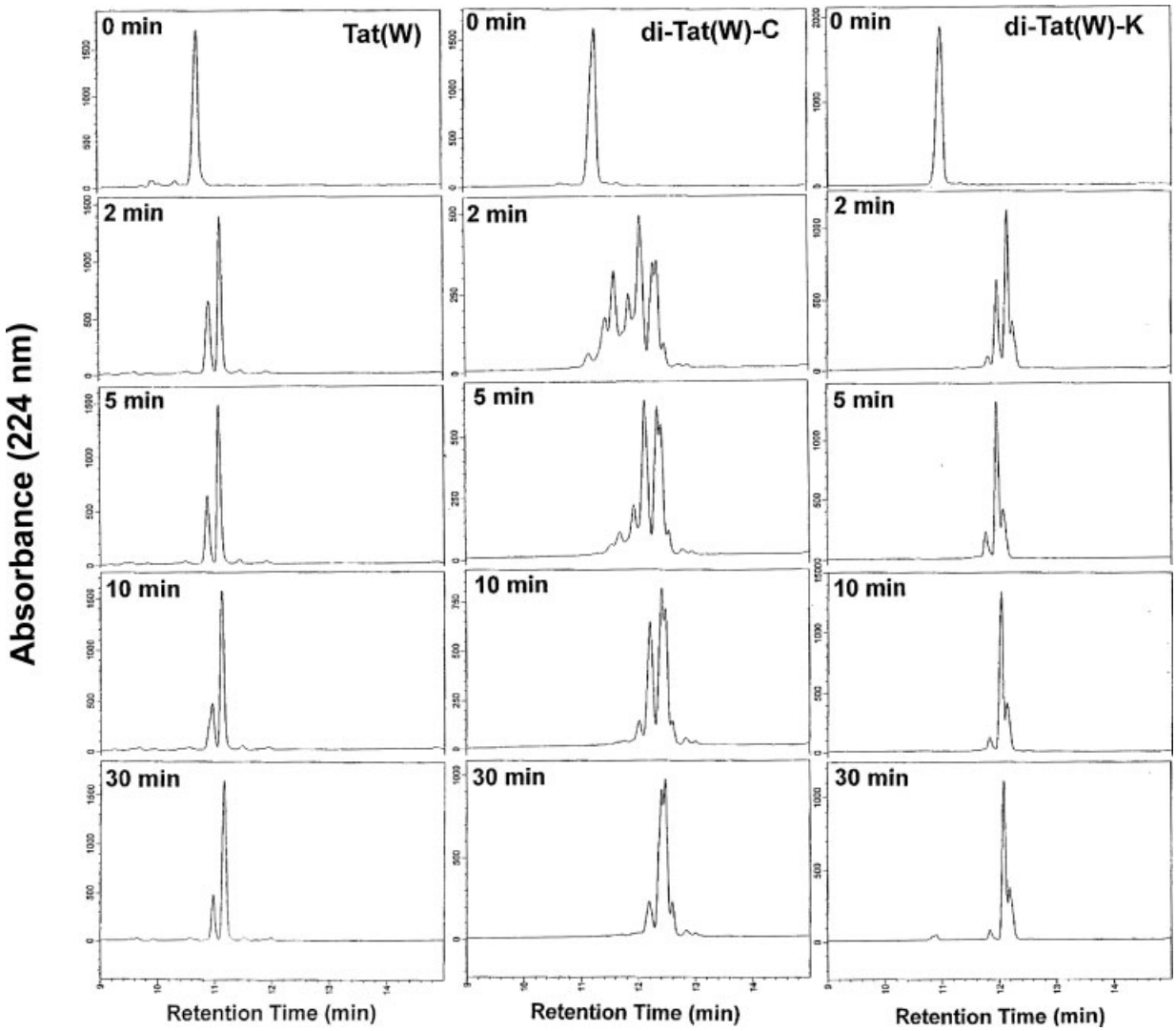

Figure 6. Proteolytic digestion of the peptides by trypsin. RP-HPLC traces of Tat(W) (A), di-Tat(W)-C (B), and di-Tat(W)-K (C) after different reaction times. Peak detection was by absorbance at 224 nm.

Journal of PeptideScience

Proteolytic Digestion

We compared the enzymatic digestion rate of the dimeric peptides [di-Tat(W)-C and di-Tat(W)-K] in aqueous solution with that of the monomeric peptide [Tat(w)]. Figure 6 shows the chromatographic traces monitoring the degradation of the peptides by trypsin over time. All peptides were completely degraded by trypsin within 2 min, indicating that the dimerization of Tat(W) does not affect the digestion rate by trypsin. Therefore, this result suggested that less translocation ability of the dimeric peptides into lipid bilayers described in Figure 5 compared with the monomeric peptide is not related to the reduction of the enzymatic digestion rate by peptide dimerization.

Discussion

It is believed that the length, charge, overall hydrophobicity, α-helicity, and amphipathic character of AMPs are responsible for their selectivity for bacterial and mammalian cells [22,23]. In addition to these parameters, the self-association (oligomerization) of AMPs in an aqueous environment is also known to be important for controlling their selectivity for specific targets [24]. In this respect, it is interesting to note that several hetero- and homodimeric AMPs stabilized by a single disulfide bond linking linear polypeptide chains have been recently discovered, namely halocidin [25], distinctin [26], and dicynthaurin [27]. Disulfide-linked dimeric peptides of halocidin [25], magainin 2 [28], and lentivirus-derived peptide [29] displayed a 4- to 20-fold increased antimicrobial activity, compared with monomeric peptides.

To investigate the effect of dimerization of a cell-penetrating peptide Tat on antimicrobial activity and mechanism of bactericidal action, a disulfide bond linked- and a Lys-branched dimeric analogs [di-Tat(W)-K and di-Tat(W)-C)] of Tat were designed and synthesized and comparatively evaluated with respect to the parental Tat. Tat(W), di-Tat(W)-C, and di-Tat(W)-K exhibited comparable antimicrobial activities against Gram-negative and Gram-positive bacteria without hemolytic activity. Furthermore, these dimeric analogs [di-Tat(W)-K and di-Tat(W)-C] displayed more rapid bactericidal activity, compared with Tat(W). This result indicates that these dimeric analogs appear to be excellent candidates for future development as novel antimicrobial agents.

Unlike common cationic α-helical AMPs with membrane-targeting mechanism, buforin II isolated from the stomach of the Asian toad *Bufo bufo* gargarizans was known to penetrate into bacterial cell membranes without inducing severe membrane perturbation and kills microorganisms by interfering intercellular functions [19,30]. Therefore, it was known that buforin II induces no or little ability in membrane depolarization of intact bacteria cells and dye leakage from bacterial-membrane-mimicking lipid vesicles [24,30–32]. Like buforin II, monomeric peptide, Tat and Tat(W) showed no or little ability in the depolarization of membrane potential of intact *S. aureus* cells and the fluorescent dye leakage of calcein-entrapped negatively charged EYPG/EYPE(7 : 3, w/w) (bacterial-membrane-mimicking lipid vesicles). On the contrary, dimeric analogs, di-Tat(W)-C, and di-Tat(W)-K significantly caused membrane depolarization and dye leakage. Furthermore, the dimeric analogs were less effectively translocated across lipid bilayers than monomeric Tat(W). These results suggest that the dimerization of Tat analog induces a partial change in the mode of its bactericidal action from intracellular target mechanism to membrane-targeting mechanism.

References

1. Boman HG, Agerberth B, Boman A. Mechanisms of action on *Escherichia coli* of cecropin P1 and PR-39, two antibacterial peptides from pig intestine. *Infect. Immun.* 1993; **61**: 2978–2984.
2. Skerlavaj B, Romeo D, Gennaro R. Rapid membrane permeabilization and inhibition of vital functions of Gram-negative bacteria by bactenecins. *Infect. Immun.* 1990; **58**: 3724–3730.
3. Sadler K, Eom KD, Yang JL, Dimitrova Y, Tam JP. Translocating proline-rich peptides from the antimicrobial peptide bactenecin 7. *Biochemistry* 2002; **41**: 14150–14157.
4. Zhao M, Weissleder R. Intracellular cargo delivery using tat peptide and derivatives. *Med. Res. Rev.* 2004; **24**: 1–12.
5. Tünnemann G, Martin RM, Haupt S, Patsch C, Edenhofer F, Cardoso MC. Cargo-dependent mode of uptake and bioavailability of TAT-containing proteins and peptides in living cells. *FASEB J.* 2006; **20**: 1775–1784.
6. Jung HJ, Park Y, Hahm K-S, Lee DG. Biological activity of Tat (47–58) peptide on human pathogenic fungi. *Biochem. Biophys. Res. Commun.* 2006; **345**: 222–228.
7. Jung HJ, Jeong K-S, Lee DG. Effective antibacterial action of Tat (47–58) by increased uptake into bacterial cells in the presence of trypsin. *J. Microbiol. Biotechnol.* 2008; **18**: 990–996.
8. Epand RF, Lehrer RT, Wang W, Maget-Dana R, Lelievre D, Epand RM. Direct comparison of membrane interactions of model peptides composed of only Leu and Lys residues. *Biopolymers* 2003; **71**: 2–16.
9. Song YM, Yang ST, Lim SS, Kim Y, Hahm KS, Kim JI, Shin SY. Effects of L- or D-Pro incorporation into hydrophobic or hydrophilic helix face of amphipathic α-helical model peptide on structure and cell selectivity. *Biochem. Biophys. Res. Commun.* 2004; **314**: 615–621.
10. Chan DI, Prenner EJ, Vogel HJ. Tryptophan- and arginine-rich antimicrobial peptides: structures and mechanisms of action. *Biochim. Biophys. Acta* 2006; **1758**: 1184–1202.
11. Schibli DJ, Epand RF, Vogel HJ, Epand RM. Tryptophan-rich antimicrobial peptides: comparative properties and membrane interactions. *Biochem. Cell Biol.* 2002; **80**: 667–677.
12. Pan Y, Wan J, Roginski H, Lee A, Shiell B, Michalski WP, Coventry MJ. Comparison of the effects of acylation and amidation on the antimicrobial and antiviral properties of lactoferrin. *Lett. Appl. Microbiol.* 2007; **44**: 229–234.
13. Thorén PE, Persson D, Isakson P, Goksör M, Onfelt A, Nordén B. Uptake of analogs of penetratin, Tat(48–60) and oligoarginine in live cells. *Biochem. Biophys. Res. Commun.* 2003; **307**: 100–107.
14. Thorén PE, Persson D, Esbjörner EK, Goksör M, Lincoln P, Nordén B. Membrane binding and translocation of cell-penetrating peptides. *Biochemistry* 2004; **43**: 3471–3489.
15. Zhu WL, Lan H, Park Y, Yang ST, Kim JI, Park IS, You HJ, Lee JS, Park YS, Kim Y, Hahm KS, Shin SY. Effects of Pro $\rightarrow$ peptoid residue substitution on cell selectivity and mechanism of antibacterial action of tritrpticin-amide antimicrobial peptide. *Biochemistry* 2006; **45**: 13007–13017.
16. Mao D, Wallace BA. Differential light scattering and absorption flattening optical effects are minimal in the circular dichroism spectra of small unilamellar vesicles. *Biochemistry* 1984; **23**: 2667–2673.
17. Barlett CR. Phosphorus assay in column chromatography. *J. Biol. Chem.* 1959; **234**: 466–468.
18. Friedrich CL, Moyles D, Beveridge TJ, Hancock RE. Antibacterial action of structurally diverse cationic peptides on gram-positive bacteria. *Antimicrob. Agents Chemother.* 2000; **44**: 2086–2092.
19. Kobayashi S, Takeshima K, Park CB, Kim SC, Matsuzaki K. Interactions of the novel antimicrobial peptide buforin II with lipid bilayers: proline as a translocation promoting factor. *Biochemistry* 2000; **39**: 8648–8654.
20. Zhu WL, Lan H, Park IS, Kim JI, Jin HZ, Hahm KS, Shin SY. Design and mechanism of action of a novel bacteria-selective antimicrobial peptide from the cell-penetrating peptide Pep-1. *Biochem. Biophys. Res. Commun.* 2006; **349**: 769–774.
21. Zhang L, Rozek A, Hancock RE. Interaction of cationic antimicrobial peptides with model Membranes. *J. Biol. Chem.* 2001; **276**: 35714–35722.

22. Giangaspero A, Sandri L, Tossi A. Amphipathic α-helical antimicrobial peptides. *Eur. J. Biochem.* 2001; **268**: 5589–5600.
23. Tossi A, Sandri L, Giangaspero A. Amphipathic, α-helical antimicrobial peptides. *Biopolymers* 2000; **55**: 4–30.
24. Zhu WL, Song YM, Park Y, Park KH, Yang ST, Kim JI, Park IS, Hahm KS, Shin SY. Substitution of the leucine zipper sequence in melittin with peptoid residues affects self-association, cell selectivity, and mode of action. *Biochim. Biophys. Acta* 2007; **768**: 1506–1517.
25. Jang WS, Kim KN, Lee YS, Nam MH, Lee IH. Halocidin: A new antimicrobial peptide from hemocytes of the solitary tunicate Halocynthia aurantium. *FEBS Lett.* 2002; **521**: 81–86.
26. Batista CV, Scaloni A, Rigden DJ, Silva LR, Rodrigues Romero A, Dukor R, Sebben A, Talamo F, Bloch C. A novel heterodimeric antimicrobial peptide from the tree-frog Phyllomedusa distincta. *FEBS Lett.* 2001; **494**: 85–89.
27. Lee IH, Lee YS, Kim CH, Kim CR, Hong T, Menzel L, Boo LM, Pohl J, Sherman MA, Waring A, Lehrer RI. Dicynthaurin: an antimicrobial peptide from hemocytes of the solitary tunicate Halocynthia aurantium. *Biochim. Biophys. Acta* 2001; **1527**: 141–148.
28. Dempsey CE, Ueno S, Avison MB. Enhanced membrane permeabilization and antibacterial activity of a disulfide-dimerized magainin analogue. *Biochemistry* 2003; **42**: 402–409.
29. Tencza SB, Creighton DJ, Yuan T, Vogel HJ, Montelaro RC, Mietzner TA. Lentivirus-derived antimicrobial peptides: increased potency by sequence engineering and dimerization. *J. Antimicrob. Chemother.* 1999; **44**: 33–41.
30. Park CB, Yi KS, Matsuzaki K, Kim MS, Kim SC. Structure–activity analysis of buforin II, a histone H2A-derived antimicrobial peptide: the proline hinge is responsible for the cell-penetrating ability of buforin II. *Proc. Natl. Acad. Sci. U.S.A.* 2000; **97**: 8245–8250.
31. Song YM, Park Y, Lim SS, Yang ST, Woo ER, Park IS, Lee JS, Kim JI, Hahm KS, Kim Y, Shin SY. Cell selectivity and mechanism of action of antimicrobial model peptides containing peptoid residues. *Biochemistry* 2005; **44**: 12094–12106.
32. Park KH, Park Y, Park IS, Hahm KS, Shin SY. Bacterial selectivity and plausible mode of antibacterial action of designed Pro-rich short model antimicrobial peptides. *J. Pept. Sci.* 2008; **14**: 876–882.

